1.1 AIRCRAFT MEASUREMENTS OF TURBULENCE: LENGTH SCALES, SPECTRA, BUDGETS, AND THE PREDICTION PROBLEM

Owen R. Coté*, Air Force Research Laboratory (AFRL), Space Vehicles Directorate, Hanscom AFB, John Roadcap, AFRL, Space Vehicles Directorate, Hanscom AFB, Donald E. Wroblewski, Boston University, Boston, MA, Ronald J. Dobosy, NOAA/ERL/ARL, Oak Ridge, Timothy L. Crawford, NOAA/ERL/ARL, Idaho Falls,

1. Prologue

The authors gratefully acknowledge the enabling contributions Dr. Timothy Crawford made to these aircraft turbulence measurements and analyses. This work could not have been done without his scientific vision, unique engineering skills, and remarkable management ability.

2. Introduction.

The goal of our direct airborne measurements of turbulence is to investigate the structure and dynamics of strong clear air and refractive turbulence layers and determine what would be required in a model to predict the evolution of such strong layers. We tried to obtain measurements in turbulence layers that were between 250 to 650 meters thick with peak C_W^2 values $\geq 10^{-1}$ $m^{1/3}/sec^2$ and C_T^2 values between 10^{-3} and 10^{-2} $deg^2/m^{2/3}$. The predictor that guides the scheduling of measurement missions in the 7 to 14.5 km altitude range is the presence of layers with bulk gradient Richardson number less than 0.4 derived from current radiosonde data within the local flight operations area.

The turbulence measurements were made with the GROB 520T EGRETT, a high altitude aircraft owned and operated by Airborne Research Australia (ARA). EGRETT was equipped with three NOAA/FRD built BAT turbulence sensors. The BAT probe is a 13 cm diameter pressure hemisphere with nine measurement ports. A micro-bead thermistor for total temperature measurement is mounted in the central dynamic pressure port. For the most recent campaign a faster NOAA/FRD thermocouple temperature sensor was mounted on top of the BAT probe. The BAT probe was designed for use on aircraft without inertial navigation systems. Each probe contains a GPS receiver and three component accelerometers. For a more complete description of the BAT probe see Crawford and Dobosy (1992). A more recent description is available on the web site: http://www.noaa.inel.gov/frd/Capabilities/BAT/.

The three BAT probes on EGRETT were mounted with one under each wing and one at the top of the tail. The use of three probes was a response to several problems relative to high altitude turbulence measurements. The first is the averaging time problem discussed by Lumley and Panofsky (1964), and Wyngaard (1973). The second problem is flow distortion. It is hoped that the multiple probes will help in the identification of flow distortion affects on spectra. The final problem is to obtain measurements of vertical gradients of mean horizontal wind and mean potential temperature with comparable accuracy to the turbulence estimates. Both measurements are used to compute Richardson number and in evaluating budgets of heat flux , temperature variance, turbulent velocity components, and Reynolds stress.

2. Where and When to Measure for Turbulence.

To determine where to measure, in what season, and at what altitudes in order to capture the dynamics of strong turbulence layers is a very difficult problem. There are several new web sites that give forecasts of regions of expected clear air turbulence. US and Global predictions are available for commercial aviation altitudes on the NOAA Turbulence Index site: (http://orbit-net.nesdis.noaa.gov/arad/fpdt/tifcsts.html). Multi-year climatology available on that site favors the south coast of Australia and Japan in their winter season. Using the climate data available on the web site: (http://www.cdc.noaa.gov/HistData/), we also concluded that it would be best to measure in winter subtropical jet stream near the south coast of Japan in February and the south coast of Australia in August.

The turbulence measurements in these locations in 1999, clearly show that turbulence in the upper troposphere and lower stratosphere is neither homogeneous or isotropic. The measurement flights where accordingly in the direction in which the atmosphere is most homogeneous, either upwind or downwind. The length of a constant altitude measurement was normally 1200 seconds, which is about 100 kilometers at EGRETT airspeed. In Japan the smallest separation of measurement levels was 660 meters and in Australia it was 330 meters.

* *Corresponding author address*: Owen R. Coté, AFRL/VSBL, 29 Randolph Rd., Hanscom AFB, MA 01731-3010; owen.cote@hanscom.af.mil

3. Measurements

The ratio of the transverse velocity structure parameters to the longitudinal velocity structure parameter should be 4/3 if the inertial sub-range is locally isotropic. In Table 1 are summarized the structure function parameters for temperature and the three velocity components for most of the measurements made in Japan in February 1999 and the 6 August 1999 measurements in Australia. On average C_V^2 is about 4/3 while C_W^2 is not which indicates an absence of local isotropy for the vertical kinetic energy component.

Also listed in the table are the ratios of pairs of structure parameters such as C_U^2/ C_T^2 . Note that under Kolmororov scaling, this ratio is equal to $\alpha_1 \varepsilon/\beta_1 \chi$, the product of the kinetic energy and temperature variance dissipation ratio with the Kolmogorov spectral constant ratio. With anisotropy it is not clear that the "spectral constants" should be constant. If so dissipation cannot be derived from the spectra. In the last column are shown estimates for turbulent dissipation (ε) which are obtained from the relation: $C_U^2 = 2\ \varepsilon^{2/3}$ which be cautioned is valid only for isotropy.

On 6 August the measurement duration at level 9650 m was 3000 seconds in contrast to the other levels that day which all were for 1200 seconds. The time series for measurement flight at 9650 meters was dived into two sections. Section A is the eastern half and B is the western half. Level 9560B had the largest structure parameters EGRETT has measured to date. The corresponding vertical accelerometer data for section B was intermittently $\pm$ 1.5 g.

In figure 1 are vertical profiles (log plot) for C_T^2, one from Japan and the one from 6 August in Australia. With the 660 meter separation between measurement levels in Japan it is possible that the peak value was not sampled. To capture the structure of the narrow turbulence layers measurements should be closer to 200 meter separation or less in the vertical when extreme turbulence is encountered. Figure 2 contains the vertical profiles of the three components of velocity variance, temperature variance, and the vertical heat flux magnitude (note log plot of amplitude masks thinness of layer). Figure 3 contains the three Reynolds stress components in a linear plot that better sets off the turbulent layer. The curvature of the <uw> profile in the turbulent layer cannot be evaluated. If present the sign of the curvature would control whether the feedback of turbulence on mean vertical gradient of the mean wind that produces negative <uw> is positive or negative.

At low spatial wave-numbers, velocity and temperature spectra follow a k_1^{-3} power law and preliminary analysis with the scaling suggested by Lumley (1964) and Weinstock (1978) indicates a non-constant spectral constant in agreement with the aircraft turbulence measurements of Lilly and Lester (1974). This is an interesting result and is also found in EGRETT measurements by the University of Wales Aberstywyth in 2000 and 2001.

In Table two are presented various key turbulent parameter ratios and scale calculations. The first column the measured magnitude of "L" $=(C_T^2/(\partial\Theta/\partial z)^2)^{3/4}$. This is the magnitude of the critical length scale that would collapse all C_T^2 profiles with $\partial\Theta/\partial z$ scaling for fluctuating temperature. Note that there are similar length scales for the velocity structure parameters. The column $<\theta^2>/w^2>$, the ratio of temperature variance to vertical velocity variance, is used to calculate L_E^2/ L_B^2, the vertical heat flux Richardson number. The magnitude of which relative to unity indicates the dynamic role of the correlation of temperature with vertical gradient of fluctuating pressure. There are two columns for flux and gradient Richardson number and one for their rato K_H /K_m. The last column is the integral scale obtained from $((u^2+ v^2 +w^2)/2)^{3/2}/\varepsilon = q^3/\varepsilon$.

4. Scales, Budgets, and Diagnostic Predictors

TEMPERATURE VARIANCE BUDGET

$\partial \langle\theta^2\rangle/\partial t$ **=** **-** advection **-** $\langle w\theta\rangle\, \partial \Theta/\partial z$ (1 **+** Horizontal Prod/Vertical stratification Prod **) +**
- $\partial \langle w\theta^2\rangle/\partial z$ (1 **+** Horizontal TT/Vertical TT**)** **-** χ

where χ ($\chi = \kappa\langle (\partial\theta/\partial x_t)^2\rangle$) is dissipation rate of temperature variance and TT stands for turbulent transport by third moments. The temperature structure parameter is obtained from the inertial sub-range temperature spectrum in the form

$$\Phi_T(k_1) = 1/4\ C_T^2\ k_1^{-5/3}$$

Under Kolmogorov scaling $C_T^2 = 4\ \beta_1\ \chi\ /\varepsilon^{1/3}$ and β_1 is the one dimensional Kolmogorov spectral constant. Under stationarity, horizontal homogeneity, and universal equilibrium, production and dissipation are equal so that:

$$-\langle w\theta\rangle\, \partial\Theta/\partial z = \chi = \kappa\langle (\partial\theta/\partial x_t)^2\rangle \ ;$$

To derive an equilibrium predictor for C_T^2 divide by $\varepsilon^{1/3}/ 4\beta_1$. The resulting identity evolves as follows:

$-4\beta_1 /\varepsilon^{1/3}\ \langle w\theta\rangle\, \partial\Theta/\partial z = 4\beta_1\ K_H /\varepsilon^{1/3}\ (\partial\Theta/\partial z)^2 = C_T^2$
$= 4\beta_1\ \kappa/\varepsilon^{1/3}\ \langle(\partial\theta/\partial x_i)^2\rangle = 4\beta_1\ L^{4/3}\ (\partial\Theta/\partial z)^2$

In the above identity we have approximated mean-square gradients by the square of a mean gradient times a ratio equivalent to a Reynolds

number: $K_H / \kappa \ (\partial\Theta/\partial z)^2 = \langle (\partial\theta/\partial x_i)^2 \rangle$. The basic problem in modeling C_T^2 in stable stratification is to determine the magnitude of "L"$^{4/3}$ or $4\beta K_H/\varepsilon^{1/3}$ which has the dimension of $(\text{length})^{4/3}$. This is illustrated in figure 1 in Wyngaard et. al. (1971b). In our terminology this is a graph of "L" $^{4/3}/ z^{4/3}$ versus Richadrson Number. The graph on the stable side would be a constant equal to 1 if the measured ratio $C_T^2/ (\partial\Theta/\partial z)^2$ had been scaled by "L"$^{4/3}$ rather than $z^{4/3}$. The modeling problem is to express "L" $^{4/3}$ as dynamically relevant length scales.

Under stable stratification $C_T^2/ (\partial\Theta/\partial z)^2$ is independent of z but not of "L"$^{4/3}$ which is now derived for equilibrium conditions. By definition we have

$K_H = - \langle w\theta \rangle /\partial\Theta/\partial z = - C_{w\theta}\, \sigma_w\, \sigma_\theta/\partial\Theta/\partial z$ and

"L"$^{4/3}$ /4β or $K_H/\varepsilon^{1/3} = - C_{w\theta}\, L_E\, L_{Iw}^{1/3}$ where L_{Iw} is equal to a vertical integral scale and L_E is the Ellison scale defined by $\langle \theta^2 \rangle = L_E^2 (\partial\Theta/\partial z)^2$. This scale will be shown to arise naturally in the vertical heat flux conservation equation.

An alternative form for stratification production modeling of C_T^2 is obtained by replacing the vertical gradient of potential temperature by $N^2\ \Theta_o/g$ and not replacing the vertical heat flux by an eddy diffusion coefficient as follows:

$$-4\beta_1/\varepsilon^{1/3} \langle w\theta \rangle\ \partial\Theta/\partial z = C_T^2, \quad \text{or equivalently}$$

$$-4\beta_1\ (g/\Theta_o \langle w\theta \rangle /\varepsilon)\ N^2\ (\Theta_o/g)^2\ \varepsilon^{2/3} = C_T^2$$

The dimensionless combination, $(g/\Theta_o \langle w\theta \rangle /\varepsilon)$, is sometimes assumed to be a constant equivalent to a critical Richardson number. Table 2 shows this is nearly true in strong turbulence but not in weak. Thus the relation between C_U^2 and C_T^2 which follows: $-2\beta_1\ R_{Ic}\ N^2\ (\Theta_o/g)^2\ C_U^2 = C_T^2$ when used in analyses of radar data to derive C_U^2 or $\varepsilon^{2/3}$ from radar C_N^2 can, with the exception of strong turbulence layers, overestimate the magnitude of ε.

VERTICAL HEAT FLUX BUDGET

$$\partial\langle w\theta\rangle/\partial t = - \text{advection} - \langle w^2 \rangle\ \partial\Theta/\partial z\ (1 + HP/VSP -$$

$$g/\Theta\ \langle \theta^2 \rangle/VSP + 1/\rho_o \langle \theta\partial p/\partial z\rangle/VSP) + 2\Omega\cos\varphi\ \langle u\theta \rangle -$$

$$\partial\langle w^2\theta\rangle/\partial z\ (1 + HTT/VTT) + \langle w\theta\rangle(\partial U/\partial x + \partial V/\partial y)$$

where $VSP = - \langle w^2 \rangle\ \partial\Theta/\partial z$, $g/\Theta\ \langle \theta^2 \rangle/VSP = L_E^2/L_B^2$ and $1/\rho_o \langle \theta\partial p/\partial z\rangle/VSP = C_{\theta\pi}\, L_E/L_\pi$ and the symbol π represents $(1/\rho)\partial p/\partial z$. In the stable boundary layer, Wyngaard et. al. (1971a) showed the vertical heat flux budget is a balance between a gain from stratification production ($- \langle w^2 \rangle\ \partial\Theta/\partial z$) and loss from buoyancy ($+ g/\Theta\ \langle \theta^2 \rangle$) and the fluctuating pressure term ($- 1/\rho_o \langle \theta\partial p/\partial z \rangle$. The ratio of buoyancy to stratification production is equivalent to L_T^2/ L_B^2 where $\langle w^2 \rangle / N^2 = L_B^2$. For measurements at the Boulder Tower under conditions of stable stratification, Hunt et. al. (1985) found this ratio was 0.64 for all cases. In the 6 Aug clear air turbulence event this ratio was between 1.7 and 4.0 for the four strong turbulence levels. However its magnitude is less than 1.0 If the ratio L_E^2/ L_B^2 is computed with filtered data containing only inertial range variance. This result implies that pressure gradient temperature correlation is a loss in the <wθ> budget and consistent with the Kansas and Boulder boundary layer results already noted. This result has implication for wave-turbulence interactions and also for closure assumptions in turbulence modeling of the upper atmosphere.

5. Conclusions

EGRETT measurements clearly show that clear air and refractive turbulence under strong stratification should be sought in the strong shear layers (≥ .03 Hz.) found above and below the jet core of the winter sub-tropical jet stream in both hemispheres.

Local anisotropy, as represented by C_w^2 /C_u^2 - the ratio of vertical to longitudinal turbulence, is not present when this ratio is less than 1.33. Egrett measurements show this is sometimes as small as 0.1, but has not yet been observed as ≥ 1. One of the more significant results to come out of the EGRETT measurements is the anisotropy of the turbulent velocity components at inertial sub-range scales while still exhibiting the characteristic -5/3 spectral power law behavior .

Turbulence data, represented by flux Richardson number and L_E^2/ L_B^2 are needed to characterize the turbulence. More investigation of wave-turbulence interaction and the role of the correlation fluctuating vertical pressure gradient with temperature (any scalar) and fluctuating vertical velocity are also needed.

6. References

Derbyshire, S. H. 1993: Local scaling in a simulated stable boundary layer. In *Waves and Turbulence Stably Stratified Flows* (Ed.) S. D. Mobbs and J. C. King. Clarendon Press. Oxford, 465 pp.

Crawford, T. L. and R. J. Dobosy, 1992: A sensitive fast-response probe to measure turbulence and heat flux from any airplane. *Boundary Layer Meteorol.* **59,** 257-278.

Hunt, J. C. R., J. C. Kaimal and J. E. Gaynor. 1985: Some observations of turbulence structure in stable layers. *Quart. J. R. Met., Soc.,* **111,** 793-815.

Lilly, D. K. and P.F. Lester. 1974: Waves and turbulence in the stratosphere. *J. Atmos. Sci.,* **31**, 800-812

Lumley, J. L. 1964: The spectrum of nearly inertial turbulence in a stably stratified fluid. *J. Atmos. Sci.***21,** 99-102.

Quirrenbach A. 1999: Observing through the turbulent atmosphere. *Principles of Long Baseline Steller interferometry*, Ed. P.R. Lawson, NASA Michelson Summer School Notes, JPL Publication 00-009 07/00, 338pp.

Weinstock, J. 1978: Vertical turbulent diffusion in a stably stratified fluid. *J. Atmos. Sci*., **35**, 1022-1027

Wyngaard, J. C. 1973: On surface-layer turbulence in *Workshop on Micrometeorology.* D. A. Haugen (Ed.) American Meteorology Society, Boston, 392pp.

_____, O. R. Cote and Y. Izumi 1971a: Local free convection, similarity, and the budgets of shear stress and heat flux., *J. Atmos. Sci.,* **28**, 1171-1182.

_____, Y. Izumi and S.A. Collins, Jr. 1971b: Behavior of the refractive-index-structure parameter near the ground. *J. Opt. Soc. Amer.***6**

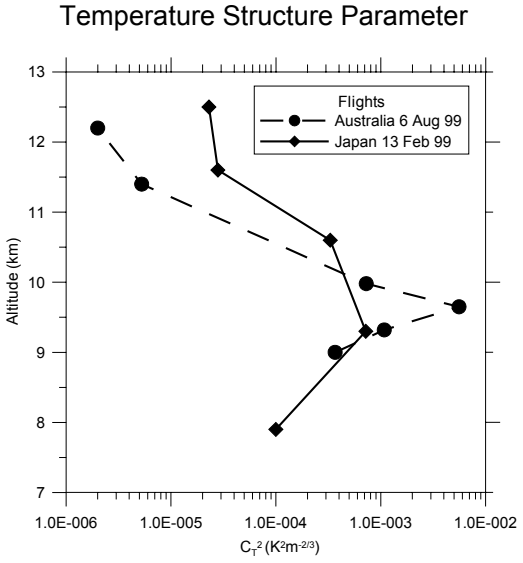

Figure 1. Vertical Profiles of Temperature Structure Parameter.

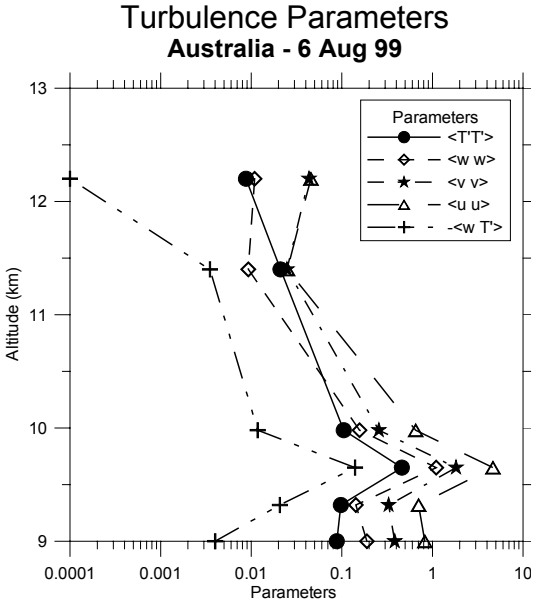

Figure 2. Vertical profiles of temperature variance, turbulent velocity components, and the vertical heat flux (multiplied by –1).

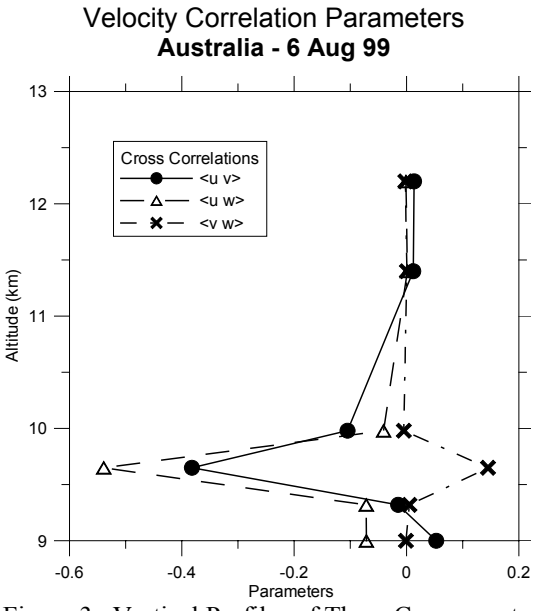

Figure 3. Vertical Profiles of Three Components of Reynolds Stress.

Table 1. Structure function parameters and ratio

Date	Altitude	C_T^2	C_u^2	C_w^2	C_v^2	Cu2/Ct2	Cw2/Ct2	Cw2/Cu2	Cv2/Cu2	ε
Japan	(meters)									(m^2/s^3)
12-Feb-99	11,849	1.40E-04	1.20E-03	5.90E-04	1.50E-03	8.6	4.2	0.49	1.25	1.47E-05
	9,231	1.60E-05	1.60E-03	1.30E-04	2.60E-03	100.0	8.1	0.08	1.63	2.26E-05
	8,932	1.25E-06	7.00E-05	1.70E-05	5.80E-05	56.0	13.6	0.24	0.83	2.07E-07
	7,694	1.50E-05	3.00E-04	1.60E-04	1.30E-03	20.0	10.7	0.53	4.33	1.84E-06
13-Feb-99	12,537	0.23E-04	9.00E-05	2.30E-05	1.40E-04	3.9	1	0.26	1.56	3.02E-07
	11,580	0.28E-04	5.60E-03	9.30E-04	4.50E-03	200.0	33.2	0.17	0.80	1.48E-04
	10,595	3.30E-04	4.20E-03	2.40E-03	4.60E-03	12.7	7.3	0.57	1.10	9.62E-05
	9,325	**7.20E-04**	3.60E-03	1.76E-03	5.30E-03	5.0	2.4	0.49	1.47	7.64E-05
	7,898	1.00E-04	**1.00E-02**	1.10E-03	1.30E-02	100.0	11	0.11	1.30	**3.54E-04**
22-Feb-99	12,343	1.40E-05	3.90E-03	4.10E-04	4.80E-03	278.6	29.3	0.11	1.23	8.61E-05
	12,362	1.70E-05	5.00E-04	2.70E-04	5.00E-04	29.4	15.9	0.54	1.00	3.95E-06
	11,751	2.50E-04	4.00E-03	2.70E-03	5.10E-03	16.0	10.8	0.67	1.27	8.94E-05
	9,850	1.60E-05	?	7.40E-05	?	?	4.6	?	?	?
	9,242	0.750E-05	1.20E-04	2.75E-05	7.50E-05	16.0	3.7	0.23	0.63	4.65E-07
23-Feb-99	12,282	2.70E-05	1.70E-04	6.60E-05	2.20E-04	6.3	2.4	0.39	1.29	7.84E-07
	11,662	0.90E-05	2.10E-03	1.00E-03	3.80E-03	233.3	111	0.48	1.81	3.40E-05
	10,243	7.00E-05	**1.20E-02**	5.50E-03	1.15E-02	171.4	78.6	0.46	0.96	**4.65E-04**
	9,969	3.30E-05	2.60E-04	7.20E-05	3.30E-04	7.9	2.2	0.28	1.27	1.48E-06
	9,536	5.70E-05	1.40E-03	5.70E-04	1.80E-03	24.6	10.8	0.41	1.29	1.85E-05
Australia										
6-Aug-99	12,200	2.00E-06	5.30E-05	2.05E-05	5.33E-05	26	10	0.38	1	1.36E-07
	11,400	5.26E-06	1.68E-04	3.94E-05	5.20E-04	319	7.5	0.23	1.26	7.70E-07
	9,980	7.27E-04	1.79E-02	1.03E-02	2.30E-02	24.6	14	0.58	1.3	8.45E-04
A	9,650	3.66E-04	1.34E-02	5.75E-03	1.48E-02	36.6	16	0.43	1.1	5.48E-04
B	9,650	**5.57E-03**	**1.20E-01**	**1.00E-01**	**1.31E-01**	21.5	18	0.83	1.1	**1.47E-02**
	9,320	1.08E-03	3.42E-02	1.80E-02	3.43E-02	31.5	17	0.52	1	2.24E-03
	9,000	3.67E-04	1.90E-02	1.16E-02	2.66E-02	51.8	32	0.61	1.4	9.26E-04

Table 2 Summary of turbulence measurements for 6 August 1999.

Altitude	"L" = $(C_T^2/(\partial\Theta/\partial z)^2)^{3/4}$	$g/\Theta\ w\theta/\varepsilon$	θ^2 / w^2	$(L_E / L_B)^2$	Flux Ri	Gradient Ri number	K_H / K_M Inverse Turb Prandtl No.	$L_I = q^3/\varepsilon$ meters
9000	4.4	0.124	0.465	1.9	.03	.07	.41	632
9320	10	0.06	0.682	2.7	.04	.07	.55	202
B 9650	34	0.27	0.418	1.7	.37	.33	1.1	500
9980	33	0.40	0.668	4.0	.40	.32	1.2	456
11400	0.6	125	2.26	10	24.8	42	.6	6.4 km
12200	0.3	139	0.8	6.9	6.4	5.5	1.1	82 km